RESEARCH MEMORANDUM

for the

U. S. Air Force

INVESTIGATION IN THE LANGLEY FREE-FLIGHT TUNNEL OF THE LOW-SPEED STABILITY AND CONTROL CHARACTERISTICS OF A 1/10-SCALE MODEL SIMULATING THE CONVAIR F-102A AIRPLANE

By Peter C. Boisseau

Langley Aeronautical Laboratory
Langley Field, Va.

NATIONAL ADVISORY COMMITTEE
FOR AERONAUTICS
WASHINGTON

14

NATIONAL ADVISORY COMMITTEE FOR AERONAUTICS

RESEARCH MEMORANDUM

for the

U. S. Air Force

INVESTIGATION IN THE LANGLEY FREE-FLIGHT TUNNEL OF THE LOW-SPEED STABILITY AND CONTROL CHARACTERISTICS OF A 1/10-SCALE MODEL SIMULATING THE CONVAIR F-102A AIRPLANE

By Peter C. Boisseau

SUMMARY

An investigation of the low-speed, power-off stability and control characteristics of a 1/10-scale model simulating the Convair F-102A airplane has been made in the Langley free-flight tunnel. The model in its basic configuration and with two modifications involving leading-edge slats and an increase in vertical-tail size was flown through a lift-coefficient range from 0.7 to the stall. Only relatively low-altitude conditions were simulated.

The longitudinal stability characteristics of the model were considered satisfactory for all conditions investigated. The lateral stability characteristics were considered satisfactory for the basic configuration over the lift-coefficient range investigated, except near the stall, where large values of static directional instability caused the model to be directionally divergent. An 80-percent increase in vertical-tail area increased the angle of attack at which the model became directionally divergent. The longitudinal and lateral control characteristics were generally satisfactory. Although the adverse sideslip characteristics for the model were considered acceptable over the angle-of-attack range, analysis indicates that the adverse sideslip characteristics of the airplane may be objectionable at high angles of attack.

INTRODUCTION

An investigation of the low-speed stability and control characteristics of a 1/10-scale model simulating the Convair F-102A airplane has been made in the Langley free-flight tunnel at the request of the U. S. Air Force. The F-102A airplane is a turbojet-powered, interceptor-type airplane with a 60° delta wing and a 60° delta vertical tail. It differs from the Convair YF-102 airplane of reference 1 by having a longer fuselage, a longer tail moment arm, a drooped leading edge which increases the wing area slightly, and chordwise fences at the 65 percent wing semispan station. These changes were made to the free-flight-tunnel model of the YF-102 from specifications furnished by Convair in September 1953. Any changes to the full-scale airplane subsequent to this date were not incorporated in the free-flight-tunnel model.

The investigation included flight tests of the model in its basic configuration and with several modifications involving leading-edge slats and an increase in vertical-tail size. Force tests of these configurations were also made to determine the static stability characteristics.

In order to permit a better interpretation of the free-flight-tunnel tests in terms of the full-scale airplane, a comparison was made between the results of force tests at a low Reynolds number (0.83×10^6) in the free-flight tunnel and force tests made by Convair at a higher Reynolds number (3.316×10^6).

SYMBOLS

All stability parameters and coefficients are referred to the stability system of axes originating at the center of gravity. A sketch showing the axes and the positive directions of the forces, moments, and angles is given in figure 1.

S	wing area, sq ft
S_t	exposed vertical-tail area, sq ft
$\bar{c}$	mean aerodynamic chord, ft
V	airspeed, ft/sec
b	wing span, ft
q	dynamic pressure, lb/sq ft

ρ	air density, slugs/cu ft
W	weight, lb
m	airplane mass, slugs
μ_b	relative-density factor, $m/\rho Sb$
β	angle of sideslip, deg
ψ	angle of yaw, relative to the tunnel axis system, deg
ϕ_1	for flight-test data, the angle between the projection of the Y-axis of the model on the YZ-plane of the tunnel and the Y-axis of the tunnel, deg
α	angle of attack, deg
η	inclination of principal longitudinal axis of airplane with respect to flight path, positive when principal axis is above flight path at the nose, deg
I_X	moment of inertia about longitudinal body axis, mk_X^2, slug-ft^2
I_Y	moment of inertia about lateral body axis, mk_Y^2, slug-ft^2
I_Z	moment of inertia about normal body axis, mk_Z^2, slug-ft^2
K_X	radius of gyration about longitudinal body axis, ft
K_Y	radius of gyration about lateral body axis, ft
K_Z	radius of gyration about normal body axis, ft
X	longitudinal force, lb
Y	lateral force, lb
Z	normal force, lb
M	pitching moment, lb-ft
N	yawing moment, lb-ft
L	rolling moment, lb-ft

C_L lift coefficient, Lift/qS

C_D drag coefficient, Drag/qS

C_m pitching-moment coefficient, M/qS$\bar{c}$

C_n yawing-moment coefficient, N/qSb

C_l rolling-moment coefficient, L/qSb

C_Y lateral-force coefficient, Y/qS

$C_{Y_\beta} = \frac{\partial C_Y}{\partial \beta}$ per deg

$C_{n_\beta} = \frac{\partial C_n}{\partial \beta}$ per deg

$C_{l_\beta} = \frac{\partial C_l}{\partial \beta}$ per deg

δ_r rudder deflection, deg

δ_e elevator deflection (elevons deflected together for elevator control), deg

δ_a aileron deflection (elevons deflected differentially for aileron control), deg

APPARATUS AND MODEL

The flight tests and static force tests were conducted in the Langley free-flight tunnel, which is designed to test free-flying dynamic models. A complete description of the tunnel and its operation is presented in reference 2. Force tests were made with a sting-type support system and an internally mounted strain-gage balance.

The 1/10-scale model used in the investigation was obtained by modifying the original Convair YF-102 model used in the investigation of reference 1 so that it approximated the fuselage shape and accurately represented the other geometrical changes of the revised design, such as fuselage length, vertical-tail position, leading-edge wing droop, and wing fences. A three-view drawing of the model is shown in figure 2 and a photograph of the model is shown in figure 3. Table I gives

the scaled-up mass and dimensional characteristics of the model. Midspan leading-edge slats and two different sizes of vertical tails were also tested on the model. (See fig. 2.) The vertical tails tested were the basic tail $\left(\frac{S_t}{S} = 0.10\right)$ and a tail with an 80-percent increase in area $\left(\frac{S_t}{S} = 0.18\right)$.

DETERMINATION OF STATIC STABILITY AND CONTROL CHARACTERISTICS OF FLIGHT-TEST MODEL

Force Tests To Determine Longitudinal Stability and Control

Force tests were made to determine the static longitudinal stability and control characteristics of the basic model and the model with modifications for an angle-of-attack range from 0° through the stall. All the force tests were run at a dynamic pressure of 3.63 pounds per square foot, which corresponds to an airspeed of about 55.7 feet per second at standard sea-level conditions and to a test Reynolds number of 0.83×10^6 based on the mean aerodynamic chord of 2.32 feet.

Static longitudinal characteristics of the basic and modified model are presented in figure 4. The data are presented for a center of gravity of 30.0 percent of the mean aerodynamic chord in order that comparisons can conveniently be made with the Convair YF-102 data from reference 1. The leading-edge slats of figure 2 were used on the model because they had a beneficial effect on the lateral stability characteristics at high angles of attack for the original model of the Convair YF-102 tested in the Langley free-flight tunnel (ref. 1). The data of figure 4 indicate that these slats were obviously not the optimum configuration for producing the most satisfactory longitudinal characteristics for the model of the present investigation. The data show that the slats decreased the lift-curve slope, the maximum lift coefficient, and the static longitudinal stability parameter $\left(-\frac{dC_m}{dC_L}\right)$. A comparison of the pitching-moment curves for the two conditions shows that the slats caused a slight pitch-up at the stall.

The static longitudinal stability and control characteristics of the free-flight-tunnel models of the F-102A and YF-102 are presented in figure 5. These data show that the lift-curve slopes and the maximum lift coefficient for the F-102A are greater than those of the YF-102. The increase in the maximum lift of the F-102A over that of the YF-102 can be attributed mainly to the cambered leading edge of the F-102A.

About 25 percent of the increase can be attributed to the fact that the coefficients were based on the area of the YF-102 wing, which was approximately 5 percent less than that of the F-102A wing. A comparison of the pitching-moment curves shows that the models had about the same static longitudinal stability and elevator effectiveness over the lift-coefficient range.

Force Tests To Determine Lateral Stability and Control

Force tests were made to determine the static lateral stability and control characteristics of the model with the vertical tail off and on over a sideslip range from 20° to -20° for angles of attack from 0° to 36°. These data were obtained at the same dynamic pressure and center-of-gravity location as for the longitudinal stability and control data. Presented for comparison with the free-flight-tunnel data are higher Reynolds number data obtained from tests conducted at Convair. The Convair data are presented for a center-of-gravity position of 27.5 percent of the mean aerodynamic chord.

Basic design.- The lateral-stability characteristics determined from the free-flight-tunnel tests are presented in figure 6 for the basic configuration, and a comparison of these (FFT) data and the Convair data is presented in figure 7. All free-flight-tunnel data are presented for an elevon deflection of -15°, which corresponded approximately to the deflection needed to trim at high lift coefficients. (See fig. 4.) The data of figure 6 show that the variation of the yawing-moment coefficient C_n and the rolling-moment coefficient C_l with angle of sideslip β is fairly linear up to an angle of attack of 20° for the model with vertical tail (fig. 6(b)). At an angle of attack of 24° the tail-off configuration (fig. 6(a)) shows a large increase in directional instability. This increase in negative slope of the yawing-moment curve for the tail-off configuration is also reflected in the data for the tail-on configuration at an angle of attack of 24°. At angles of attack of 26° and higher, the tail-on data show a destabilizing break in the yawing-moment curve at sideslip angles greater than approximately ±5°.

A comparison of the data of figure 7 shows that, at low and moderate angles of attack, the yawing-moment and rolling-moment curves for both models had the same general characteristics. At high angles of attack, however, the Convair data indicated less directional instability than the free-flight-tunnel data.

The data of figures 6 and 7 are summarized in figure 8 in terms of the side-force parameter C_{Y_β}, the directional-stability parameter C_{n_β}, and the effective-dihedral parameter $-C_{l_\beta}$. Since the data of figures 6 and 7 are nonlinear for some conditions, the data of figure 8 are presented at low angles of sideslip ($\beta = \pm 2°$) and high angles of sideslip ($\beta = \pm 10°$). These data indicate that the free-flight-tunnel model

had lower directional stability over the angle-of-attack range than the Convair model and also became directionally unstable at a lower angle of attack than the Convair model. Because of the nonlinearities in the yawing-moment curves, the directional stability determined for $\beta = \pm 10^\circ$ decreased to zero at an angle of attack about 2° lower than that for $\beta = \pm 2^\circ$. The effective dihedral $-C_{l_\beta}$ was positive for both models over the angle-of-attack range, with the Convair model having higher values of $-C_{l_\beta}$ at the higher angles of attack for $\beta = \pm 2^\circ$.

The yawing-moment data in figure 8 for the free-flight-tunnel model are shown for a center-of-gravity position of 27.5 percent $\bar{c}$ as well as of 30.0 percent $\bar{c}$ in order that a direct comparison may be made with the Convair data. The data indicate that changing the location of the center of gravity of the free-flight-tunnel model from 30.0 to 27.5 percent of the mean aerodynamic chord had only a slight effect on the directional stability. Changing the center of gravity from 30.0 to 27.5 percent of the mean aerodynamic chord had a negligible effect upon the rolling moment of the model.

The variation of the lateral-stability parameters C_{Y_β}, C_{n_β}, and C_{l_β} with lift coefficient and angle of attack for the F-102A are compared in figure 9 with data from reference 1 for the YF-102. In general the variation of the lateral-stability parameters with angle of attack was similar for the two models. Because of the difference in lift curves for the F-102A and the YF-102 at high angles of attack (fig. 5), the plots of C_{n_β} against lift coefficient (fig. 9) show that the directional stability drops off less abruptly for the F-102A than for the YF-102. The effective dihedral $-C_{l_\beta}$ was positive for both models over the lift-coefficient range with the F-102A model having slightly higher values of $-C_{l_\beta}$ at the higher lift coefficients.

Modified design.- In an effort to obtain satisfactory static lateral-stability characteristics at high angles of attack, force tests were made of the model with increased vertical-tail size $\left(\frac{S_t}{S} = 0.18\right)$ and with leading-edge slats. (See fig. 2.) The data obtained in these tests are presented in figures 10 and 11. The data of figure 12 compare the lateral-stability characteristics of the basic model with those of the modified model at angles of attack of 24° and 30°. The data of figures 10 and 11 are summarized in figure 13 in terms of the lateral-stability parameters C_{Y_β}, C_{n_β}, and $-C_{l_\beta}$ for angles of sideslip of $\pm 2^\circ$ and $\pm 10^\circ$.

The data of figure 12(a) show that at an angle of attack of 24°, increasing the size of the vertical tail $\left(\frac{S_t}{S} = 0.18\right)$ caused the model to

[redacted]

become directionally stable and also made the curve linear. For the basic tail the leading-edge slats produced a small increment in directional stability at low angles of sideslip and a very large increment at large angles of sideslip so that the overall result was a fairly linear variation of the yawing-moment coefficient with angles of sideslip. The slats had little effect on the directional stability when they were used in combination with the enlarged tail.

The data of figure 12(b) show that, at $\alpha = 30^{\circ}$, the model with the basic tail was directionally unstable and the model with the enlarged tail was about neutrally stable for sideslip angles of $\pm 5^{\circ}$. The model with either tail and without slats had a sharp destabilizing break at a sideslip angle of about $\pm 5^{\circ}$. The slats caused a destabilizing effect for small angles of sideslip and a large reduction in the directional instability for large angles of sideslip. The effects of increased tail size and leading-edge slats are shown more clearly in the summary data of figure 13. The aileron and rudder control effectiveness for the basic model are presented in figure 14.

FLIGHT TESTS

Flight tests were made from a lift coefficient of about 0.70 through the stall in order to determine the dynamic stability and control characteristics of the model in its basic configuration and with increased tail size and leading-edge slats. Flight tests were made at a center-of-gravity position of 27.5 percent $\bar{c}$. Light wing loadings were used in order to minimize damage to the model in crackups. The model was flown with coordinated aileron and rudder control and with aileron-alone control. Aileron deflections of $\pm 15^{\circ}$ and a rudder deflection of $\pm 25^{\circ}$ were used for all conditions. Only relatively low-altitude conditions were simulated.

The model behavior during flight was observed by a pilot situated just aft of the tunnel test section. The pilot's observations and supplementary data obtained by motion-picture records served as a basis for all discussion of the flight tests.

FLIGHT-TEST RESULTS AND DISCUSSION

Interpretation of Flight-Test Results

In interpreting the results of the model flight tests in terms of the full-scale airplane, it is necessary to consider any differences between the static stability derivatives of the model and those of the

full-scale airplane and any differences between the scaled-up mass characteristics of the model and the mass characteristics of the airplane. If there are no differences in these factors, then the airplane would be expected to exhibit dynamic characteristics similar to those of the free-flight-tunnel model.

Although no mass data were available for the full-scale airplane, the data of reference 1 show that the values of the scaled-up moments of inertia for the model of the Convair YF-102 were generally similar to those of the airplane at normal gross weight. Therefore, the mass data presented in table I for the scaled-up moments of inertia for the model of the F-102A are expected to be representative of those of the airplane at normal gross weight. It has been shown that the static stability characteristics of the free-flight-tunnel model at low Reynolds number are in fair agreement with the characteristics of the Convair model at higher Reynolds number. It is likely, however, that the abrupt changes noted in the stability parameters at high lift coefficients will occur at somewhat higher lift coefficients for the airplane than for the model. The dynamic behavior of the airplane is therefore expected to be similar to that of the free-flight-tunnel model, except that corresponding dynamic behavior might occur at higher lift coefficients.

It should be pointed out that the full-scale airplane should be easier to fly than the model because its angular velocities will be only about one-third as high as those of the model. Another factor which should facilitate the pilot's control of the airplane is the fact that he has independent aileron and rudder control rather than the coordinated aileron and rudder control which was used on the model.

In interpreting the lateral-control characteristics of models in terms of full-scale airplanes, it has been found necessary in some cases to consider the differences in piloting technique between the models and the airplanes. A free-flight-tunnel study has revealed that airplanes which have high yawing inertia and low rolling inertia, such as the F-102A, tend to execute a pure rolling motion about the principal longitudinal axis of inertia, at least during the early stages of a rolling maneuver. When these airplanes roll in this manner, an adverse sideslip angle about the stability axis is produced which is approximately equal to the angle of inclination of the principal axis times the sine of the angle of bank ($\eta \sin \phi$). For instance, for a given angle of inclination of the principal axis of 20°, an airplane of this type when banked 30° will have an angle of adverse sideslip of 10° about the stability axis. Since the pilot of a free-flight-tunnel model flies the model from a remote position and can perform only very limited maneuvers, he does not object to the model's executing essentially pure roll about the principal axis and apparently cannot detect the resulting adverse sideslip about the stability axis that might be objectionable to the pilot of the

full-scale airplane. The estimation of the adverse sideslip characteristics of the airplane based on the model flight tests is therefore expected to be optimistic.

In the discussion of the flight tests, it should be pointed out that what the pilot observes is the yaw of the model in the tunnel, except in cases of violent motions of translation. This in effect is the same as sideslip, except for sign. In the discussion that follows, the terms yaw and sideslip are used interchangeably, yaw being used to imply that the attitude in the tunnel is the significant thing at the time and sideslip being used when the aerodynamic effects of sideslip are under consideration. Similar considerations apply to the usage of angle of attack and pitch.

The results of the present investigation are illustrated more graphically by motion pictures of the flights of the model than is possible in a written presentation. For this reason a motion-picture film supplement to this paper has been prepared and is available on loan from the NACA Headquarters, Washington, D. C.

Longitudinal Stability and Control

The longitudinal stability and control characteristics of the Convair F-102A were similar to those of the Convair YF-102 and were considered satisfactory for all conditions investigated. Although the longitudinal characteristics of the model were considered to be generally satisfactory, some difficulty was encountered in flying the model in the high lift-coefficient range because of the large variation of drag with lift, which is generally a characteristic of low aspect-ratio delta wings (ref. 3). This large variation of drag with lift caused large variations of the glide angle with lift coefficient and necessitated almost continuous corrections to tunnel angle and airspeed in order to maintain flight in the tunnel.

Lateral Stability

Basic design.- In general, the lateral stability characteristics for the basic configuration of the F-102A were similar to those for the basic configuration of the YF-102 tested in reference 1. At angles of attack below about 25° the model was easy to fly and the lateral stability was considered satisfactory. The lateral (Dutch Roll) oscillations were well damped for all flight conditions. The directional stability decreased with increasing angle of attack, and at an angle of attack near the stall (α = 26°) the model became directionally divergent. A typical flight record of the model at an angle of attack of 26° is shown in figure 15(a). The model could be flown at this angle of attack as long as the pilot was

able to keep the angle of sideslip small. It appeared, however, that, once an angle of sideslip of approximately 5° was reached, the model could not be recovered and it diverged rapidly to larger angles of sideslip and snap-rolled into the tunnel wall. The directional divergence of the free-flight-tunnel model was evidently caused by the large values of the static directional instability at the higher angles of attack. The increased rate of the divergence at the moderate and large angles of sideslip is attributed to the sharp destabilizing break in the yawing-moment curve which occurred at the higher angles of attack. Another factor which might have contributed to the directional divergence was the decrease in positive effective dihedral in the higher angle-of-attack range.

As flights were attempted at angles of attack above 26°, it became more difficult for the pilot to keep the model at small angles of sideslip and the divergence became more violent. Flights attempted at an angle of attack of 30° were very short because the model diverged soon after take-off. A flight record of the model at an angle of attack of approximately 30° is presented in figure 15(a). For this case the model sideslipped to an angle greater than 30° and rolled to an angle of about 30° before crashing into the tunnel wall. More effective use of the rudder yawing moment could probably have been obtained if the rudder had been deflected independently, but even the maximum available yawing moment of the rudder would be insufficient to balance out the yawing moment due to sideslip at sideslip angles greater than approximately ±5° at an angle of attack of 30°.

In comparing the force-test data of figure 8, it is seen that the free-flight-tunnel model becomes directionally unstable at an angle of attack approximately 5° lower than that for the Convair model; this difference was probably partly caused by differences in Reynolds number. Since the flight tests showed that the free-flight-tunnel model could be flown at an angle of attack about 5° higher than that at which C_{n_β} became negative, it is possible that the airplane, because it will be operating at much higher Reynolds numbers, might not experience a directional divergence before it stalls. Other factors that might influence the high angle-of-attack behavior of the full-scale airplane are its slower yawing motions and independent rudder control which might enable the pilot to control the yawing motion fairly well and prevent a divergence in most cases, even at high angles of attack. The danger of a directional divergence will still exist, however, since the airplane might inadvertently reach the divergent conditions if the pilot becomes engrossed in some action, such as an evasive maneuver in combat.

Modified design.- Increasing the size of the vertical tail by 80 percent $\left(\frac{S_t}{S} = 0.18\right)$ did not eliminate the directional divergence but did increase the angle of attack at which the divergence occurred.

[redacted]

Flights were obtained at angles of attack up to about 33° with the enlarged tail. When flights were attempted at an angle of attack of 33° or higher, the model diverged in sideslip but the divergence was less violent than with the basic tail at lower angles of attack. Records of the model with the enlarged tail are presented in figure 15(b) for model angles of attack of approximately 30° and 33°.

The addition of leading-edge slats did not increase the angle of attack at which the model became directionally divergent. In fact, it appeared that the model diverged at a slightly lower angle of attack with slats on than with slats off. The force-test data of figure 13 show that, for sideslip angles of ±2°, the addition of the slats increased the static directional instability at angles of attack greater than about 28°. A flight record showing a directional divergence of the model for an angle of attack of approximately 33° is presented in figure 15(c). The fact that the use of slats in combination with increased tail size failed to eliminate the directional divergence of the F-102A model in the high angle-of-attack range as they had done for the YF-102 can be explained by the force-test data of figure 16. These data are for the two models with the large vertical tail and leading-edge slats and show that, at the higher angles of attack, the F-102A had much greater static directional instability and much lower effective dihedral than the YF-102. This slat configuration, which had been selected on the basis of exploratory force tests on the YF-102 model, apparently was not satisfactory for use on the F-102A model. A more suitable slat configuration for the F-102A could probably have been found from additional exploratory force tests with this model, but such tests were considered beyond the scope of this investigation.

Lateral Control

The lateral control characteristics of the basic and modified configurations were considered satisfactory over the lift-coefficient range investigated and were generally similar to those obtained for the YF-102 model in reference 1. Although the control characteristics could not be evaluated through the stall for the basic configuration, it is believed that they would be similar to those of the model with increased tail size. In flights of the model with increased tail size near the stall, some adverse sideslip with aileron alone was obtained because of the adverse yawing moments due to aileron deflection (fig. 14(a)). This adverse sideslipping was eliminated, however, by using the rudder in combination with the ailerons for coordinated control. In the higher angle-of-attack range, the model could be controlled satisfactorily until a directional divergence occurred.

As previously pointed out, full-scale flight test of airplanes which have high yawing inertia and low rolling inertia, similar to the

F-102A, indicated more severe adverse sideslip characteristics than were demonstrated by the models of these airplanes in the free-flight tunnel. It is possible, therefore, that the adverse sideslipping behavior of the full-scale airplane may be objectionable at the high angles of attack.

CONCLUSIONS

Results have been presented from a free-flight-tunnel stability and control investigation of a 1/10-scale model simulating the Convair F-102A airplane. The model was flown through a lift-coefficient range from 0.7 to the stall, and only relative low-altitude conditions were simulated. From the results, the following conclusions were drawn:

1. In general, the flight characteristics for the basic configuration of the Convair F-102A airplane model were similar to those for the basic configuration of the Convair YF-102 airplane model previously tested.

2. The longitudinal stability characteristics were considered satisfactory for the basic and modified configurations over the lift-coefficient range investigated.

3. The lateral stability characteristics for the basic configuration were considered satisfactory over the lift-coefficient range investigated except near the stall where large values of static directional instability caused the model to be directionally divergent.

4. An 80-percent increase in vertical-tail area increased the angle of attack at which the model became directionally divergent.

5. The use of leading-edge slats in combination with an 80-percent increase in vertical-tail area did not eliminate the directional divergence through the stall on the F-102A model as they did for the YF-102 model.

6. The longitudinal and lateral control characteristics were generally satisfactory. Although the adverse sideslip characteristics for the model were considered acceptable over the angle-of-attack

range, analysis indicates that the adverse sideslip characteristics of the full-scale airplane may be objectionable at high angles of attack.

Langley Aeronautical Laboratory,
National Advisory Committee for Aeronautics,
Langley Field, Va., February 7, 1955.

Peter C. Boisseau
Aeronautical Research Scientist

Approved: Thomas A. Harris
Thomas A. Harris
Chief of Stability Research Division

JKS

REFERENCES

1. Johnson, Joseph L., Jr., and Boisseau, Peter C.: Investigation of the Low-Speed Stability and Control Characteristics of a 1/10-Scale Model of the Convair YF-102 Airplane in the Langley Free-Flight Tunnel. NACA RM SL53L04, U. S. Air Force, 1953.

2. Shortal, Joseph A., and Osterhout, Clayton J.: Preliminary Stability and Control Tests in the NACA Free-Flight Wind Tunnel and Correlation With Full-Scale Flight Tests. NACA TN 810, 1941.

3. McKinney, Marion O., Jr., and Drake, Hubert M.: Flight Characteristics at Low Speed of Delta-Wing Models. NACA RM L7K07, 1948.

TABLE I

SCALED-UP MASS AND DIMENSIONAL CHARACTERISTICS OF A 1/10-SCALE MODEL SIMULATING THE CONVAIR F-102A AIRPLANE TESTED IN THE LANGLEY FREE-FLIGHT TUNNEL

Weight, lb	19,140
Wing loading, W/S, lb/sq ft	27.54
Relative density factor, μ_b	9.44
Moments of inertia:	
I_X, slug-ft^2	17,580
I_Y, slug-ft^2	119,300
I_Z, slug-ft^2	124,600
Ratios of radii of gyration to wing span:	
k_X/b	0.1426
k_Y/b	0.372
k_Z/b	0.3801
Wing:	
Airfoil	NACA 0004-65 (modified)
Area, sq ft	695
Span, ft	38.134
Aspect ratio	2.09
Root chord, ft	35.628
Tip chord, ft	0.801
Mean aerodynamic chord $\bar{c}$, ft	23.72
Longitudinal distance from leading-edge of root chord to leading edge of $\bar{c}$, ft	11.96
Sweepback of leading edge, deg	60
Sweepforward of trailing edge, deg	5
Dihedral, deg	0
Incidence, deg	0
Slats:	
Span, percent wing span (two)	31.7
Chord, ft	1.36
Elevons:	
Area behind hinge line, percent wing area (two)	10.12
Span, percent wing span (two)	69.0
Chord, parallel to fuselage reference axis:	
Root, ft	3.15
Tip, ft	2.04
Basic tail $\left(\frac{S_t}{S} = 0.10\right)$:	
Airfoil section	NACA 0004-65 (modified)
Exposed area, sq ft	68.2
Span, ft	8.66
Aspect ratio	1.1
Enlarged tail $\left(\frac{S_t}{S} = 0.18\right)$:	
Exposed area, sq ft	118.5
Span, ft	11.54
Aspect ratio	1.12
Rudder (same for both tails):	
Area, sq ft	10.54
Span, ft	5.72
Root chord, ft	2.09
Tip chord, ft	1.59

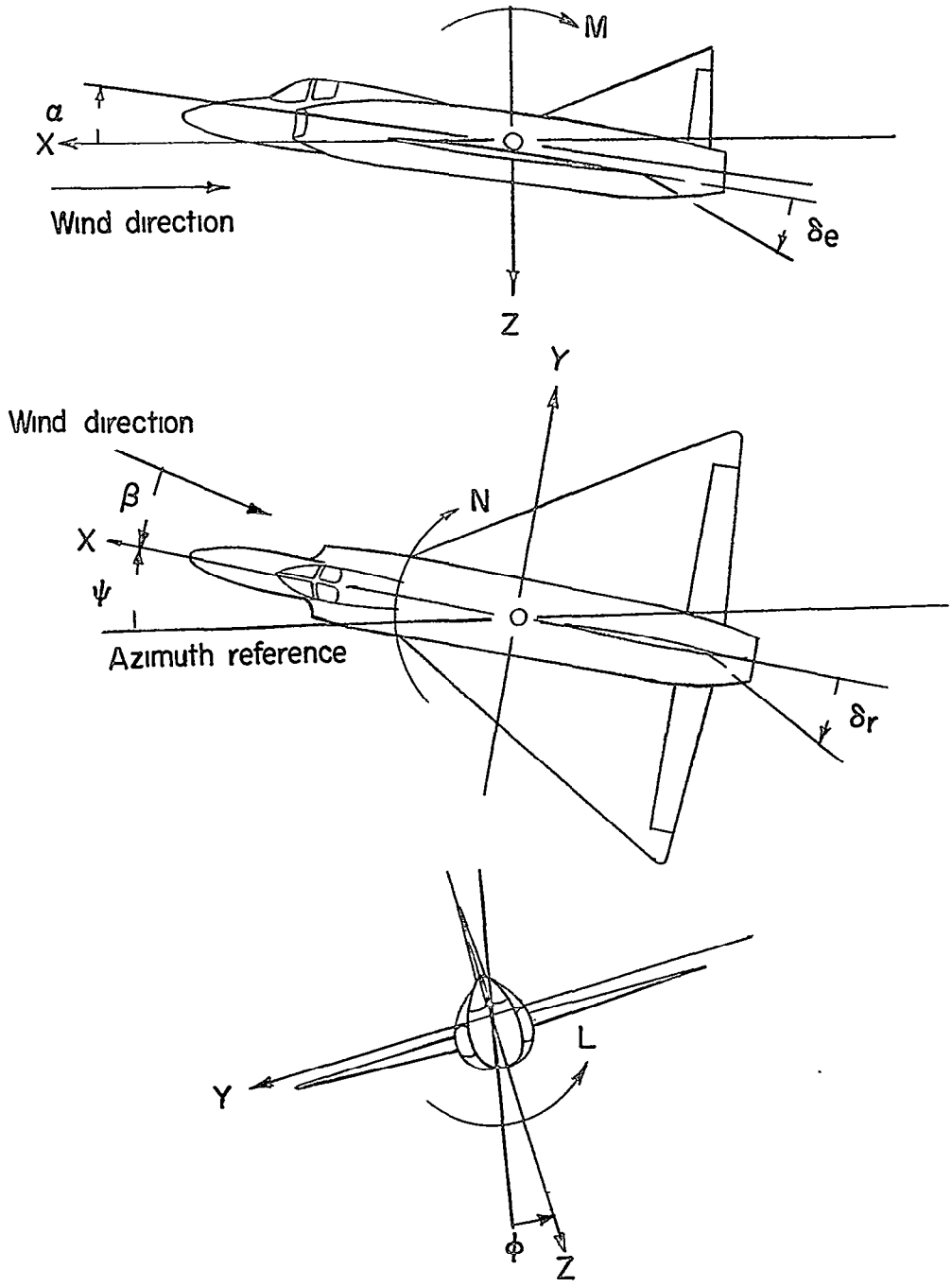

Figure 1.- The stability system of axes. Arrows indicate positive directions of moments, forces, and angles. This system of axes is defined as an orthogonal system having the origin at the center of gravity and in which the Z-axis is in the plane of symmetry and perpendicular to the relative wind; the X-axis is in the plane of symmetry and perpendicular to the Z-axis; and the Y-axis is perpendicular to the plane of symmetry. At a constant angle of attack, these axes are fixed in the airplane.

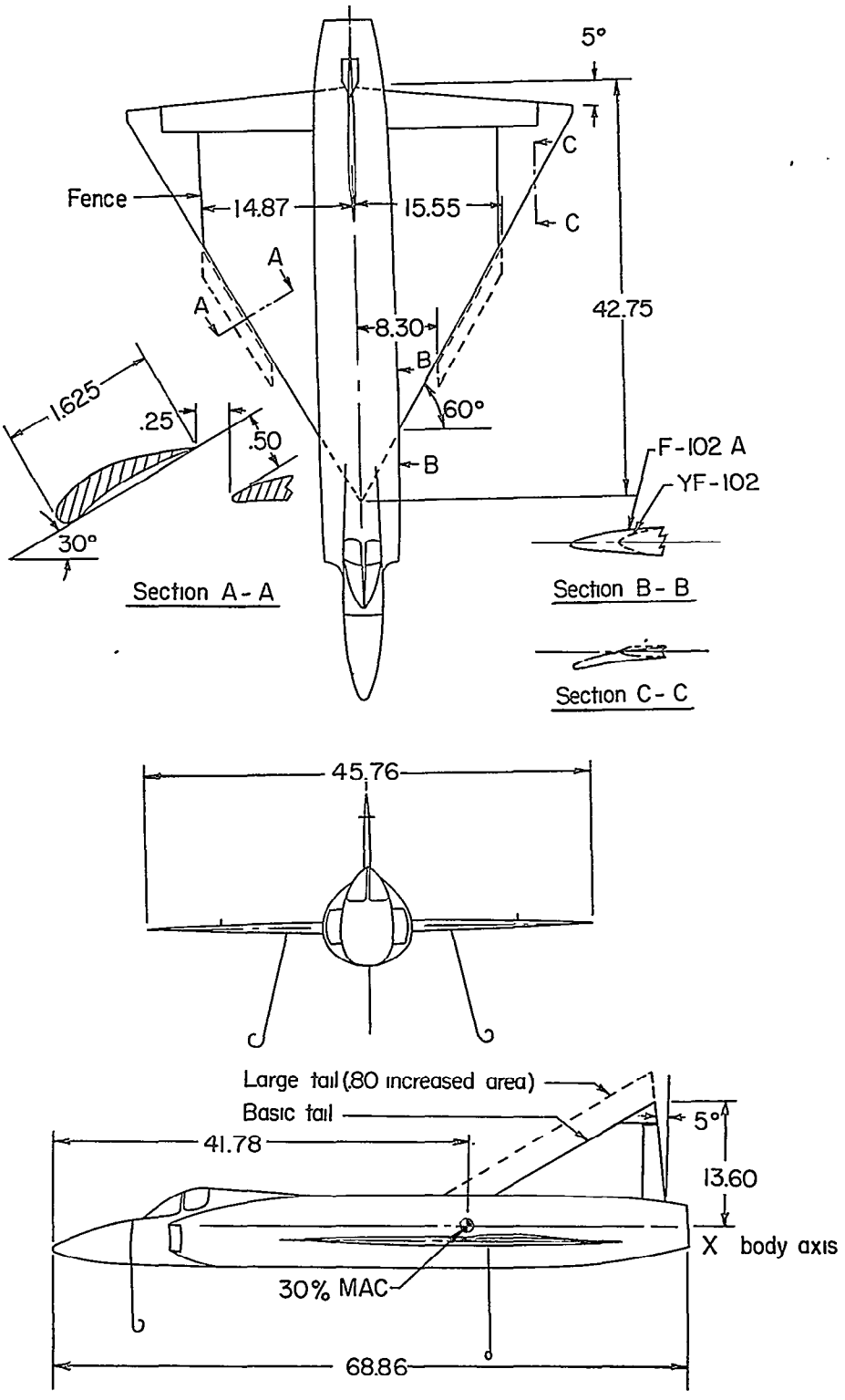

Figure 2.- Three-view drawing of a 1/10-scale model simulating the Convair F-102A airplane tested in the Langley free-flight tunnel. All dimensions are in inches.

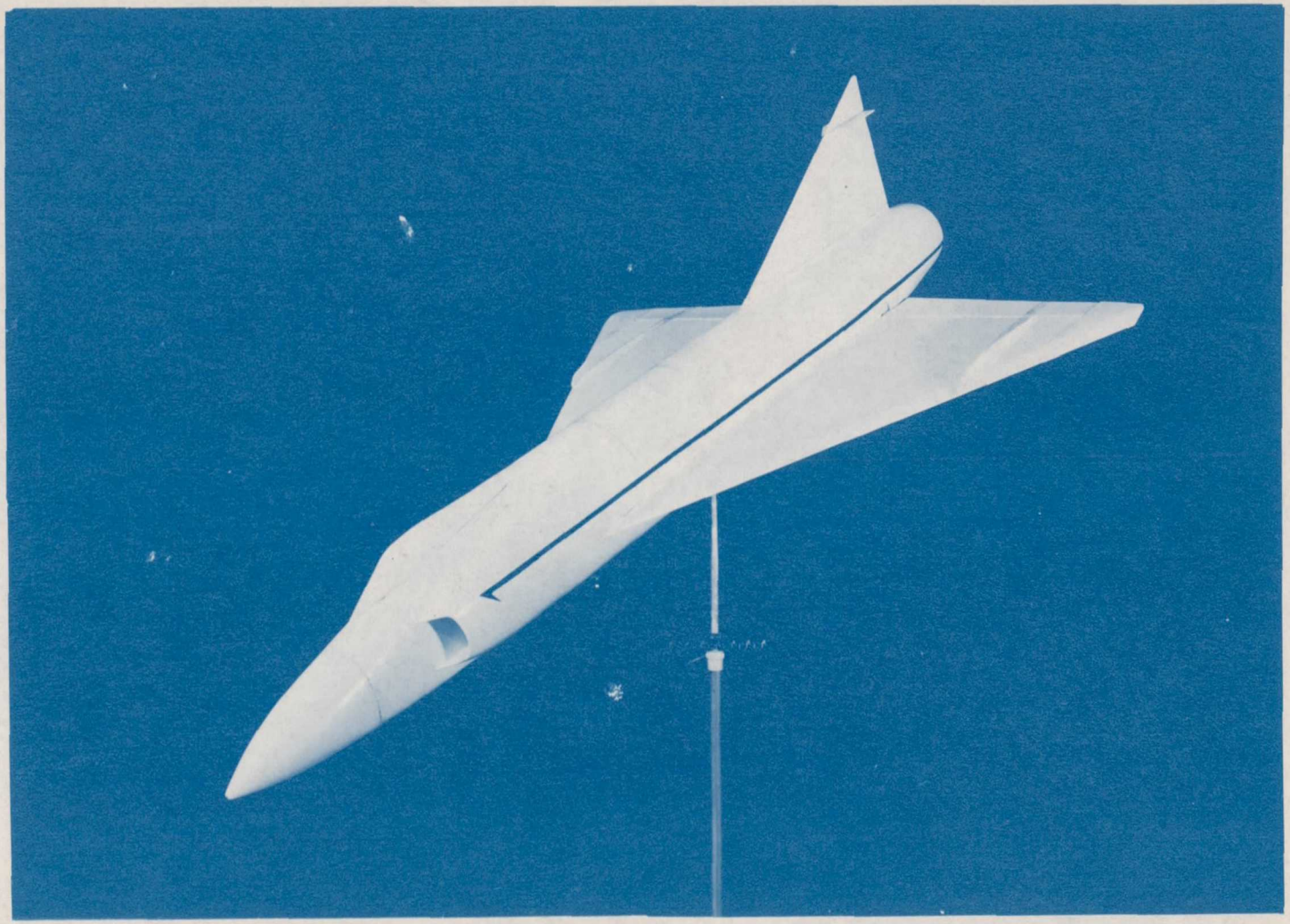

L-83396

Figure 3.- Photograph of 1/10-scale model simulating the Convair F-102A airplane tested in the Langley free-flight tunnel.

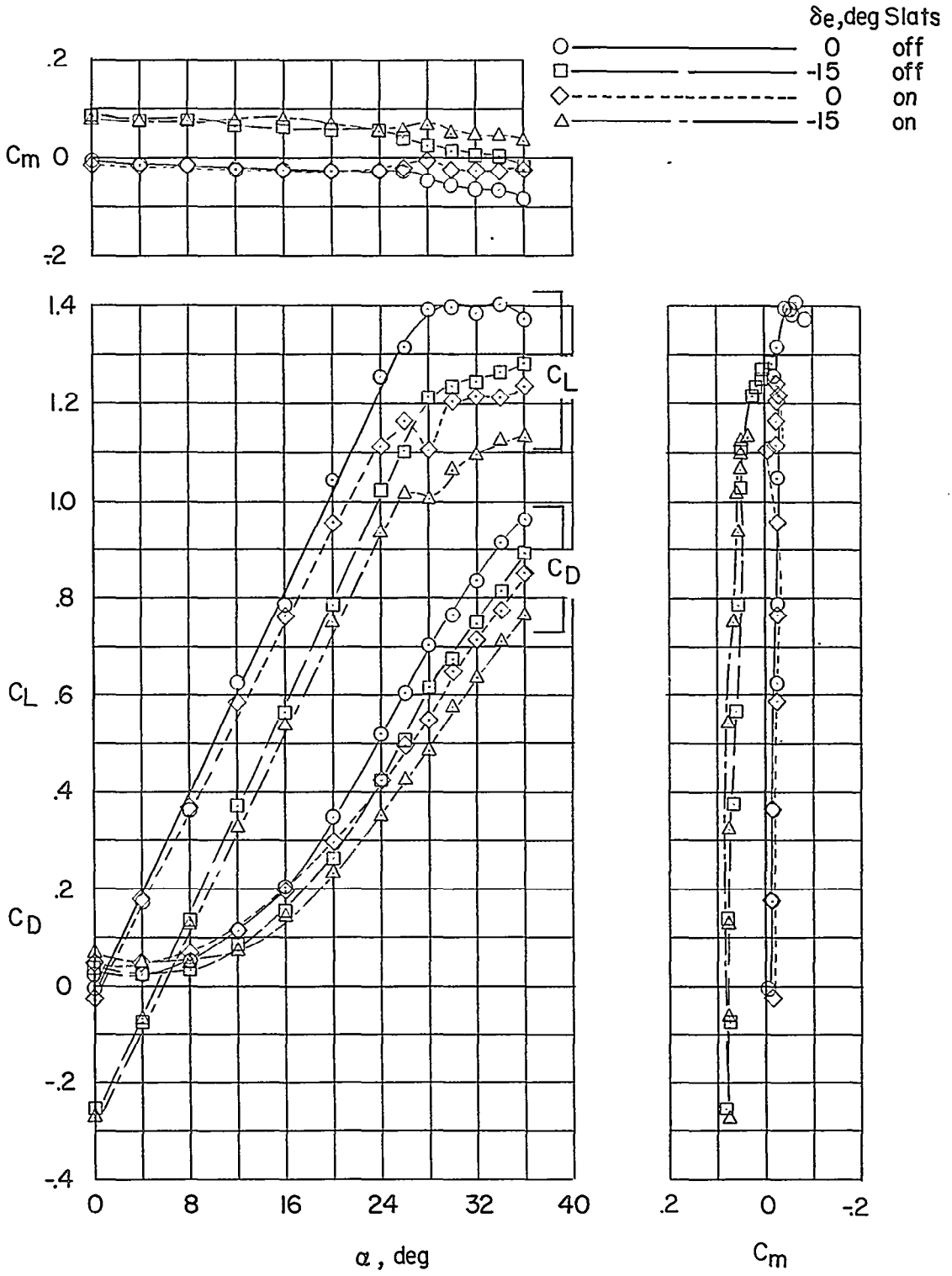

Figure 4.- Aerodynamic characteristics of a model simulating the F-102A airplane tested in the Langley free-flight tunnel. $\frac{S_t}{S} = 0.10$.

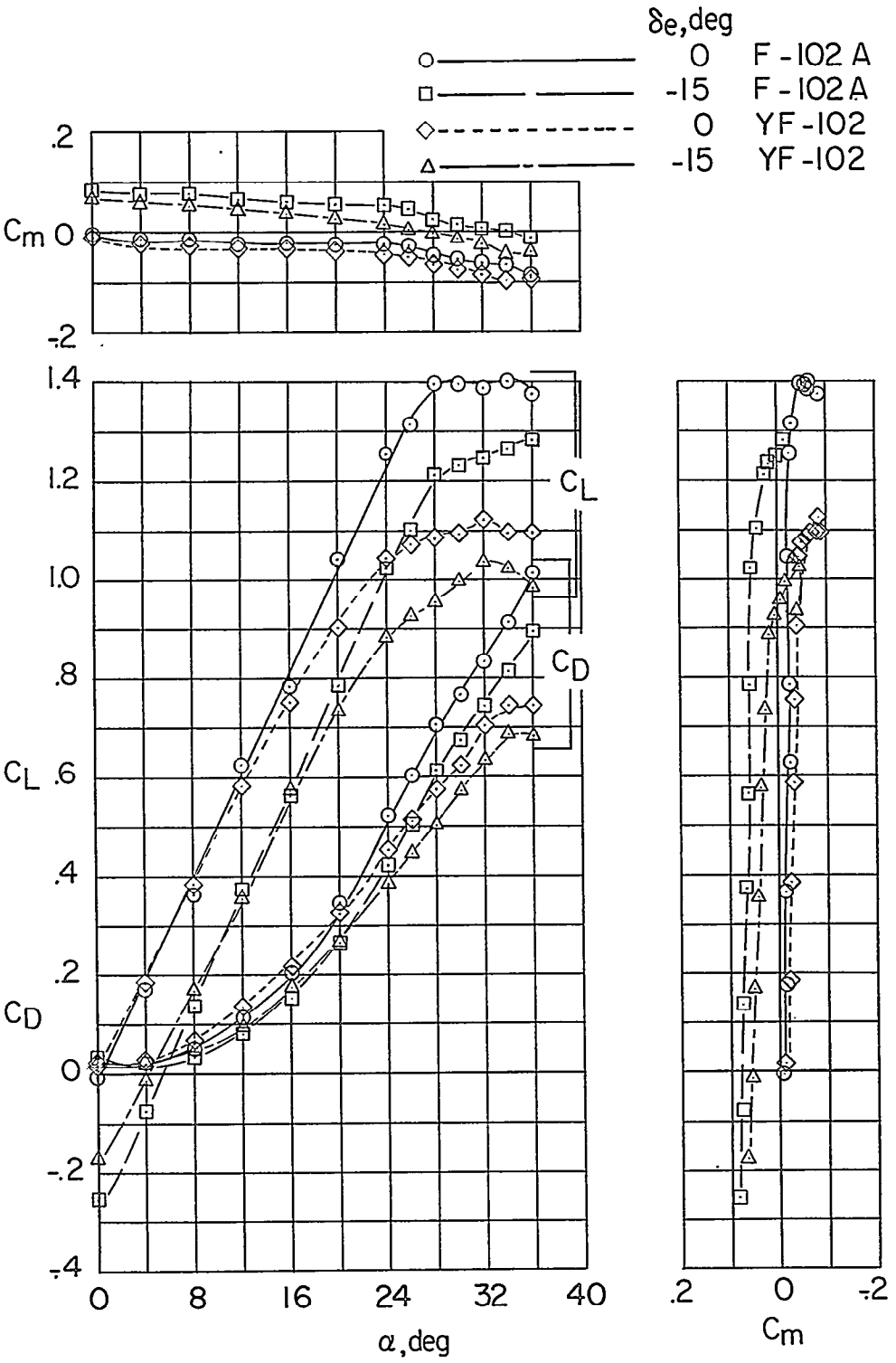

Figure 5.- Comparison of the aerodynamic characteristics of models of the F-102A and YF-102 airplanes tested in the Langley free-flight tunnel. $\frac{S_t}{S} = 0.10$.

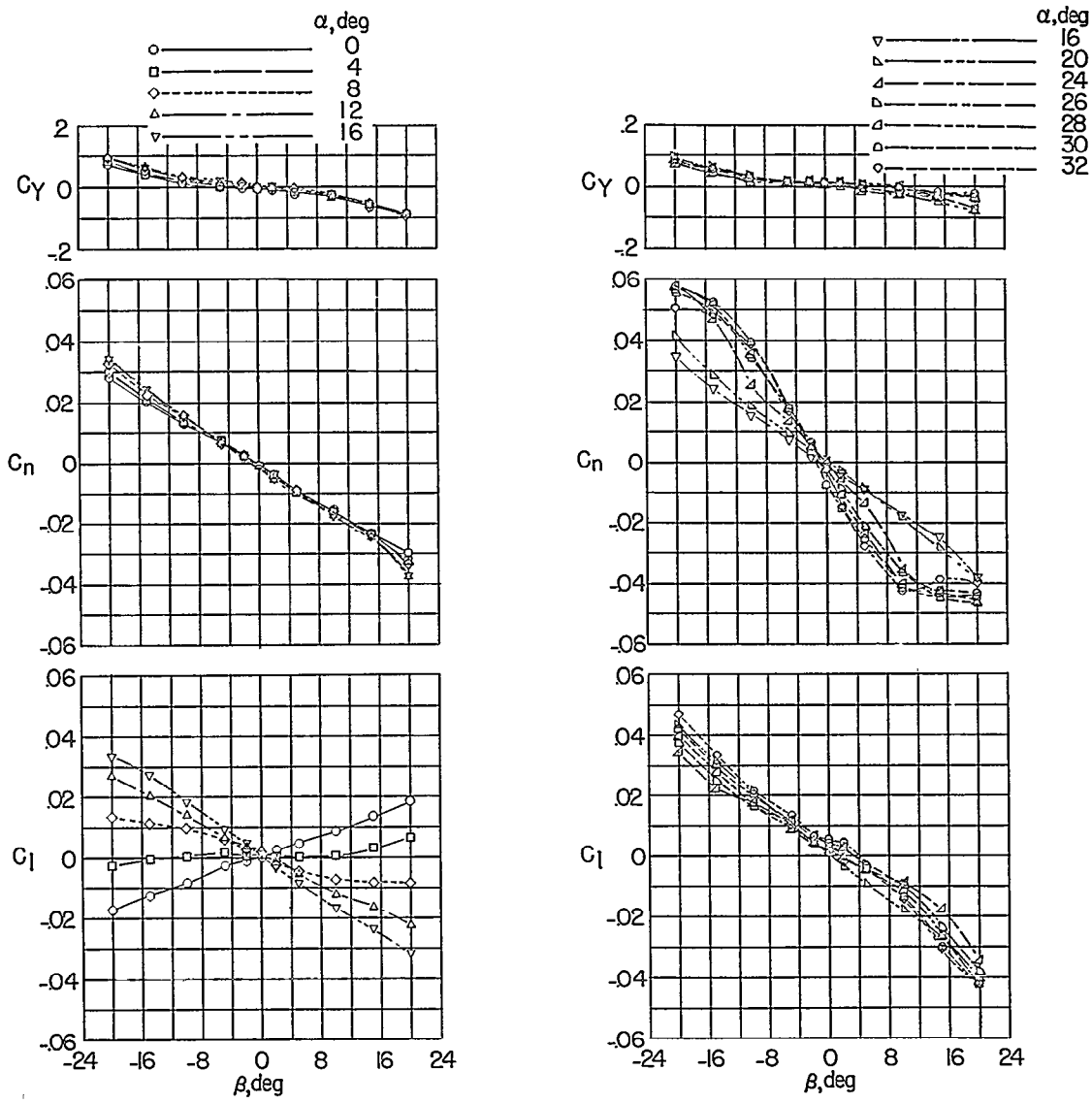

(a) Tail off $\left(\frac{S_t}{S} = 0\right)$.

Figure 6.- Lateral characteristics of the model tested in the free-flight tunnel. $\delta_e = -15°$.

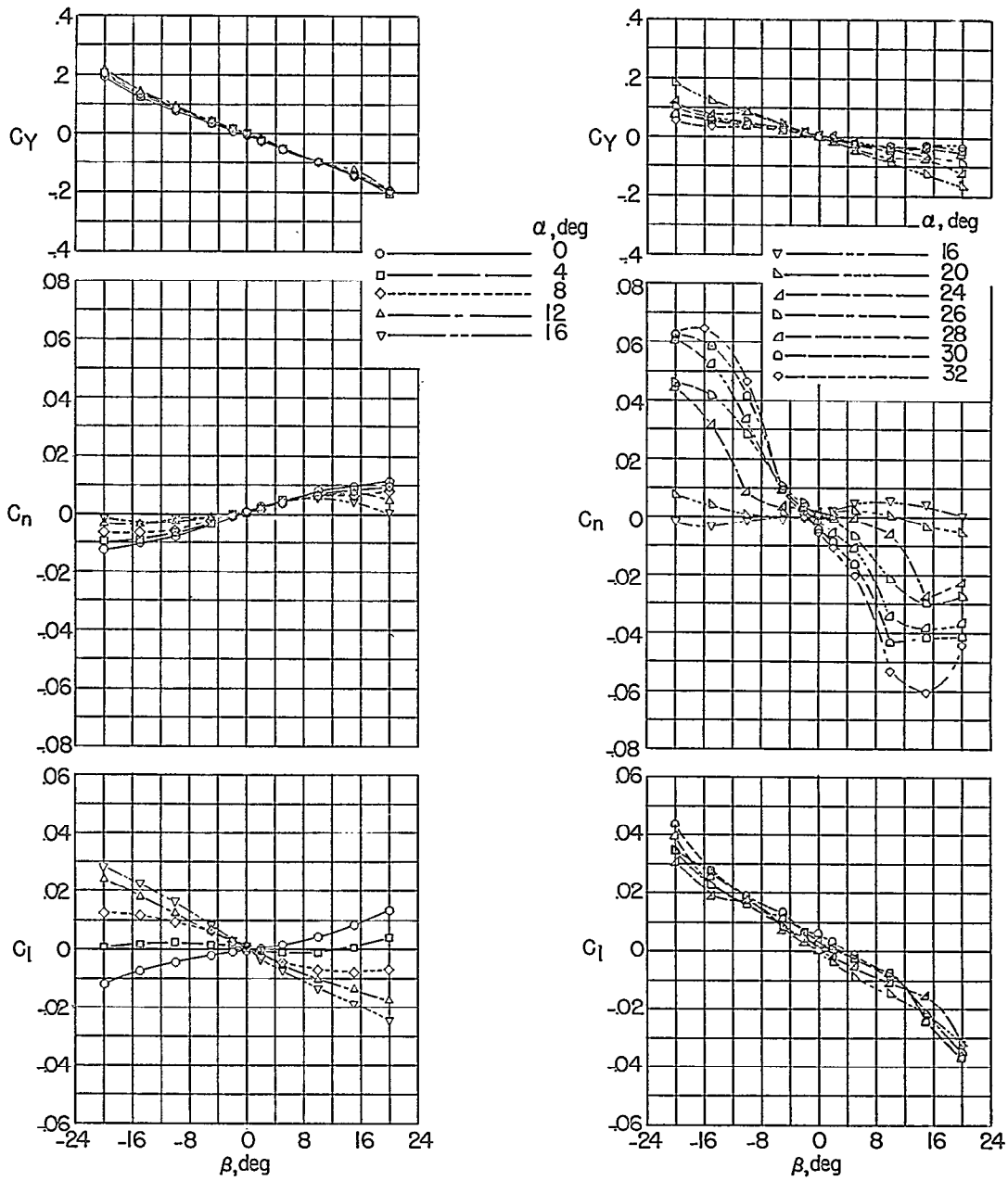

(b) $\frac{S_t}{S} = 0.10$.

Figure 6.- Concluded.

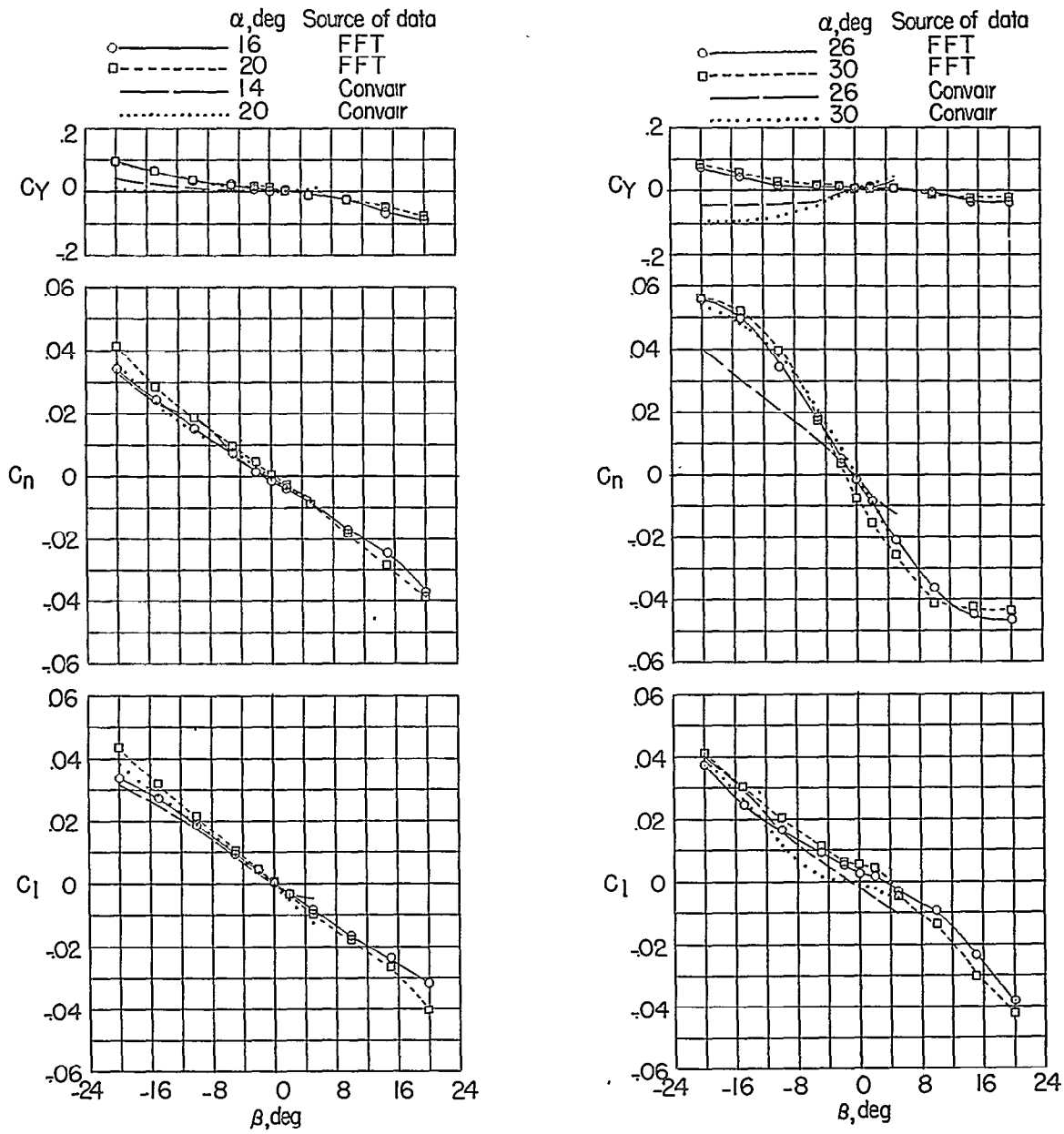

(a) Tail off $\left(\frac{S_t}{S} = 0\right)$.

Figure 7.- Comparison of lateral stability characteristics of model tested in the Langley free-flight tunnel and model tested by Convair.

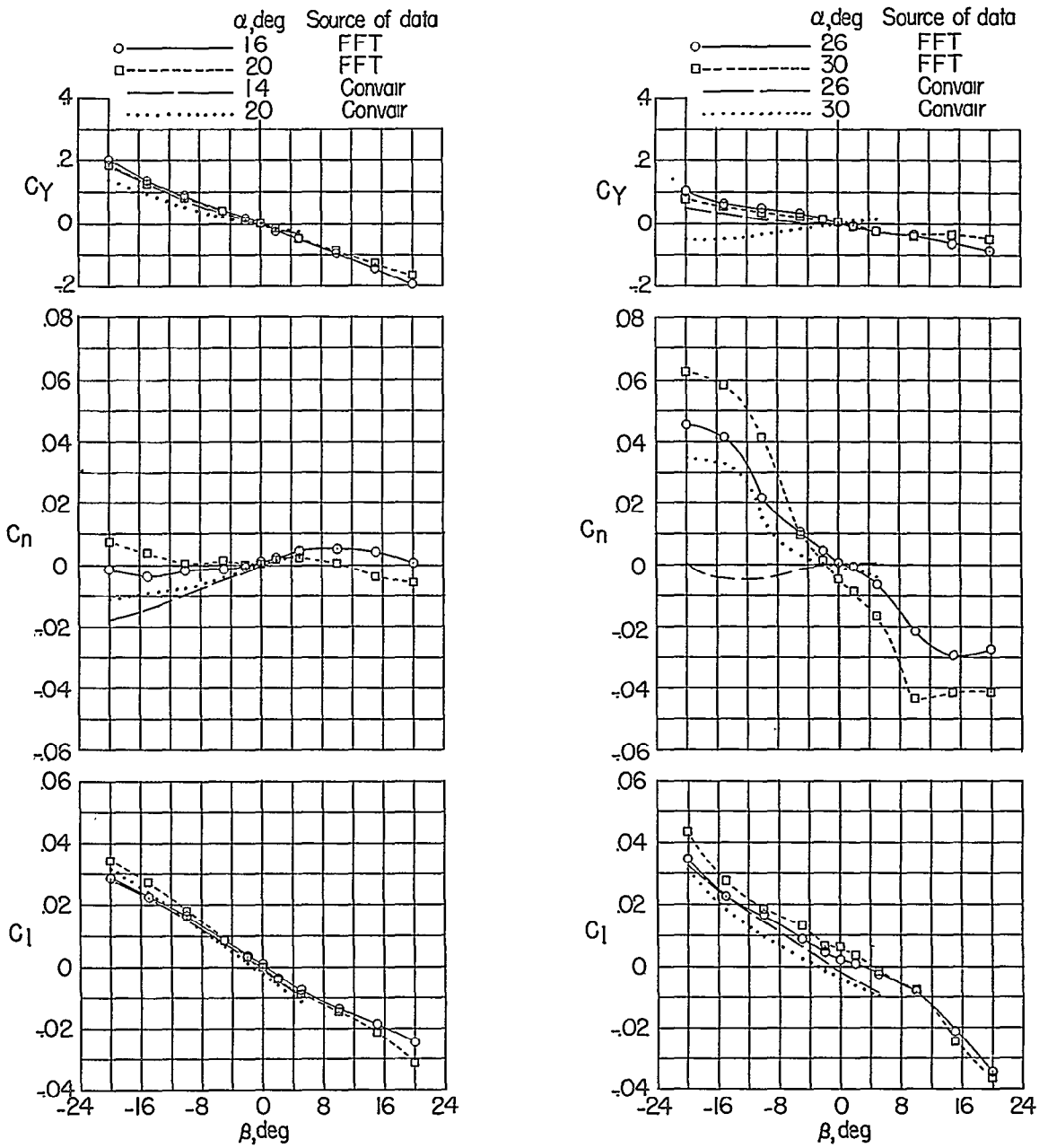

(b) $\frac{S_t}{S} = 0.10$.

Figure 7.- Concluded.

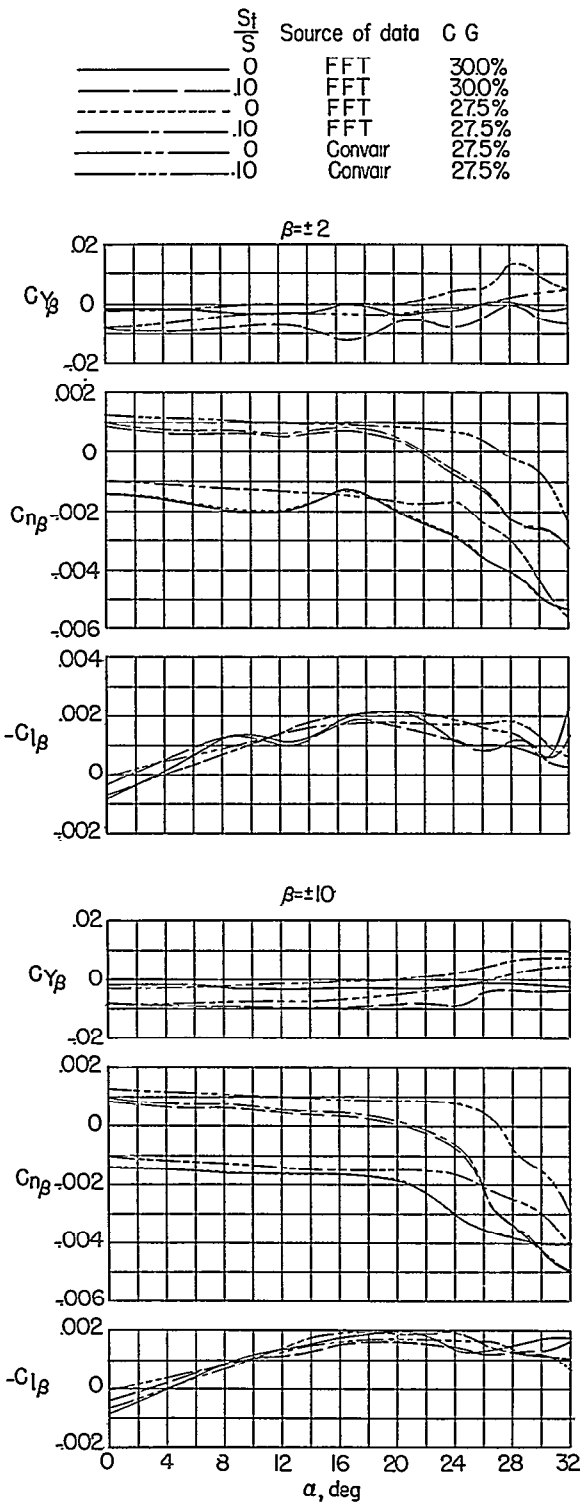

Figure 8.- Lateral-stability parameters of the model tested in the Langley free-flight tunnel and the model tested by Convair.

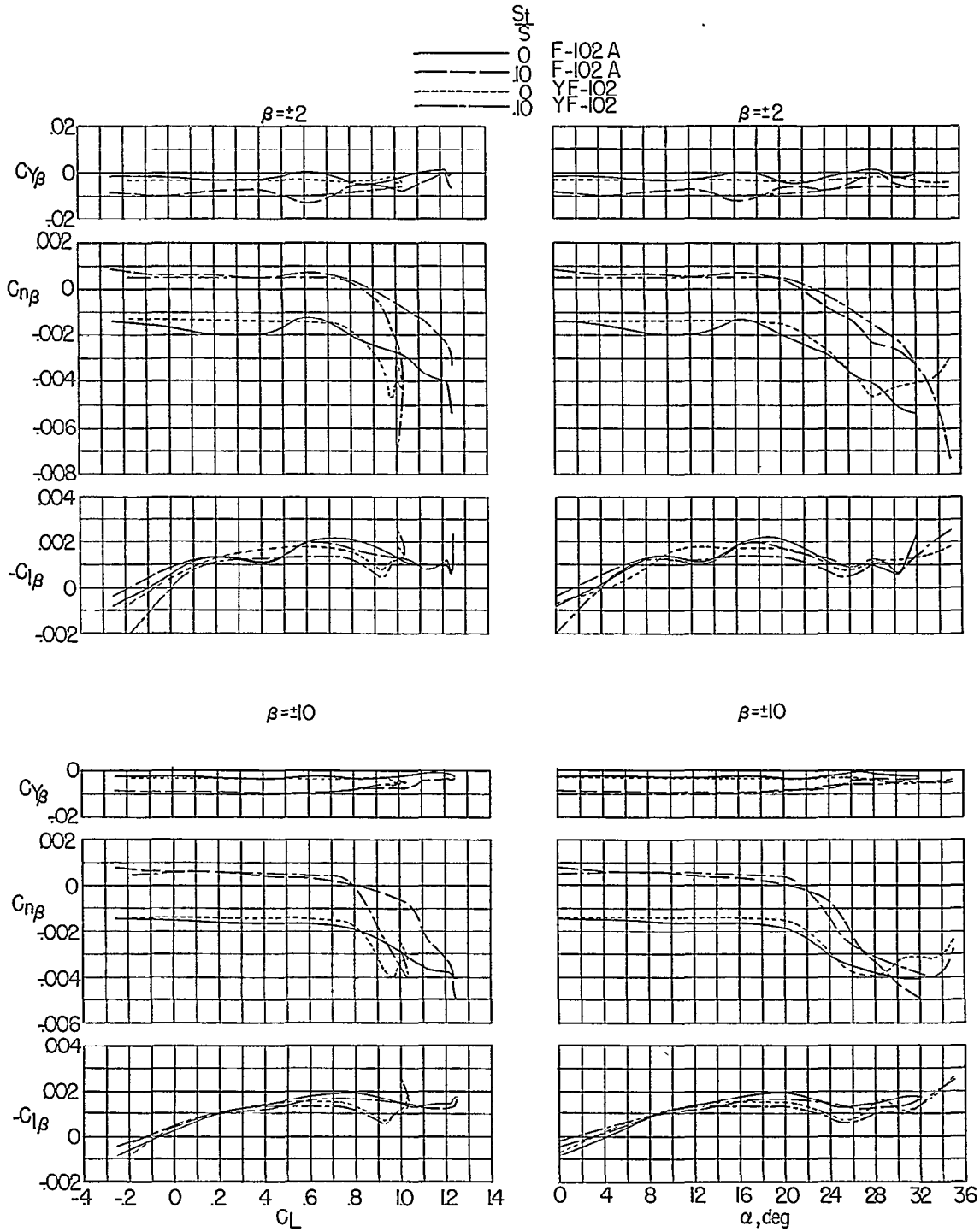

Figure 9.- Lateral-stability parameters of a model simulating the F-102A airplane and a model of the YF-102 airplane tested in the Langley free-flight tunnel. $\delta_e = -15^\circ$.

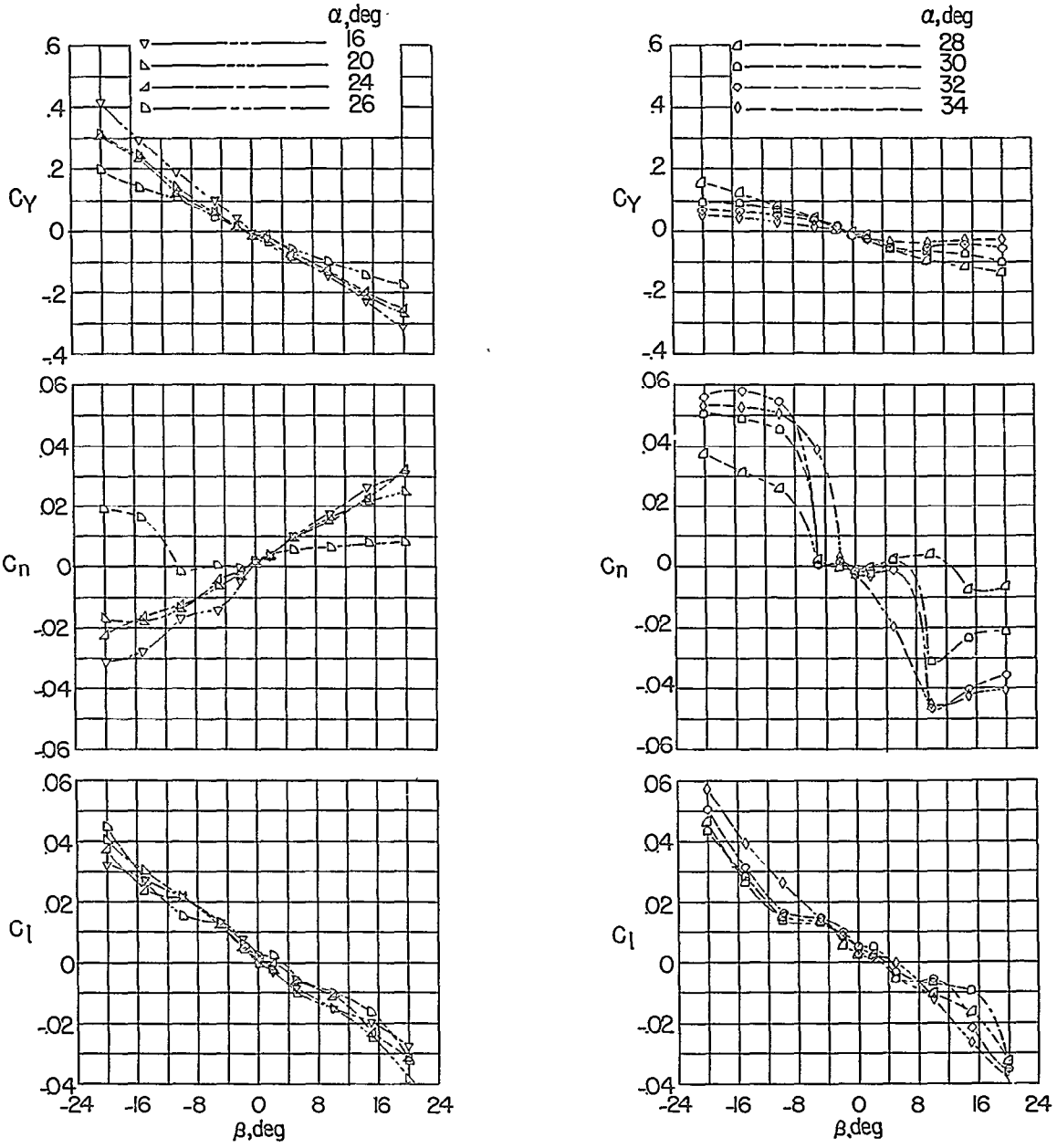

Figure 10.- Lateral characteristics of the model tested in the Langley free-flight tunnel. $\delta_e = -15^\circ$; $\frac{S_t}{S} = 0.18$.

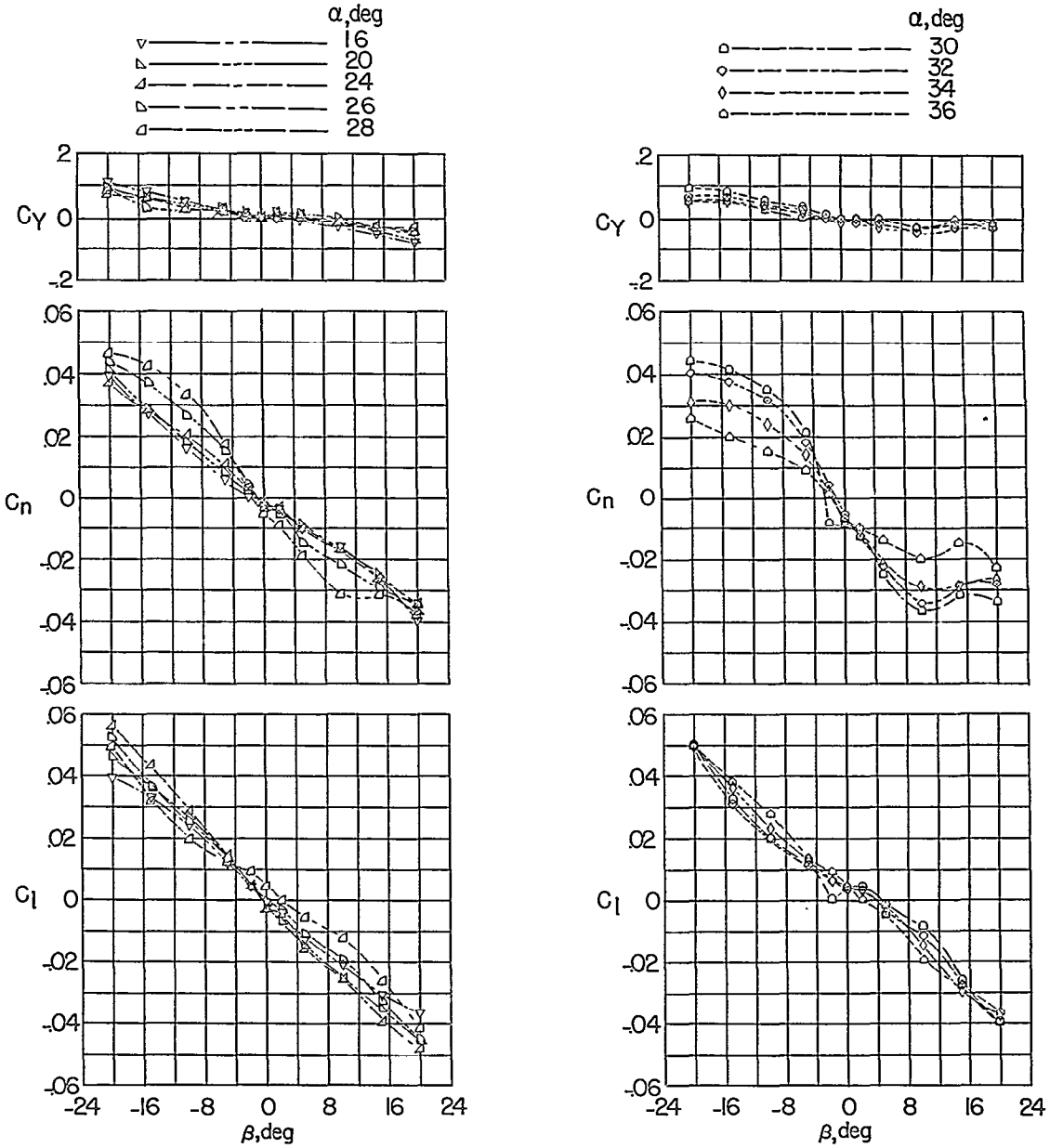

(a) Tail off $\left(\frac{S_t}{S} = 0\right)$.

Figure 11.- Lateral characteristics of the Langley free-flight-tunnel model with leading-edge slats. $\delta_e = -15^\circ$.

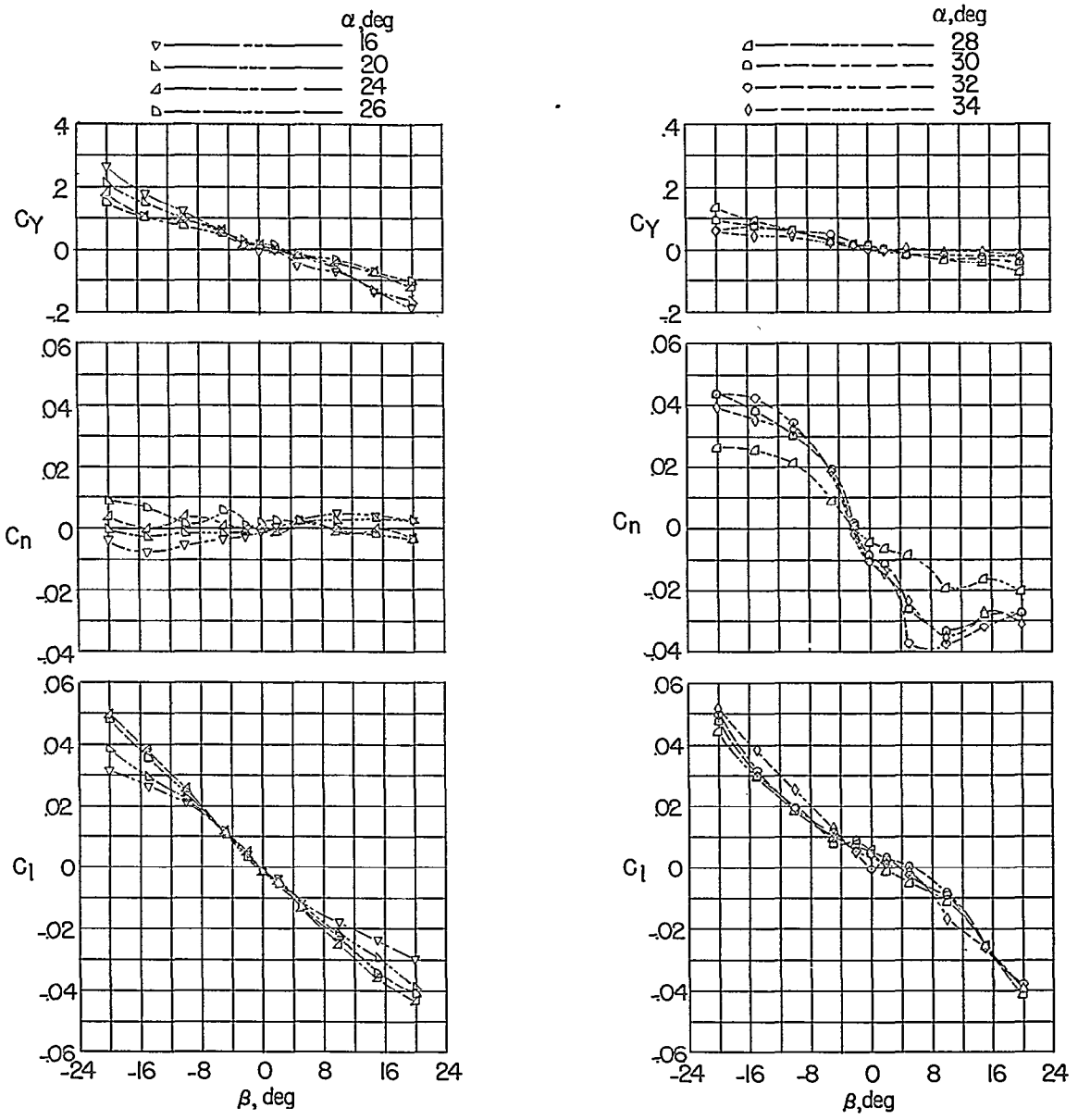

(b) $\frac{S_t}{S} = 0.10$.

Figure 11.- Continued.

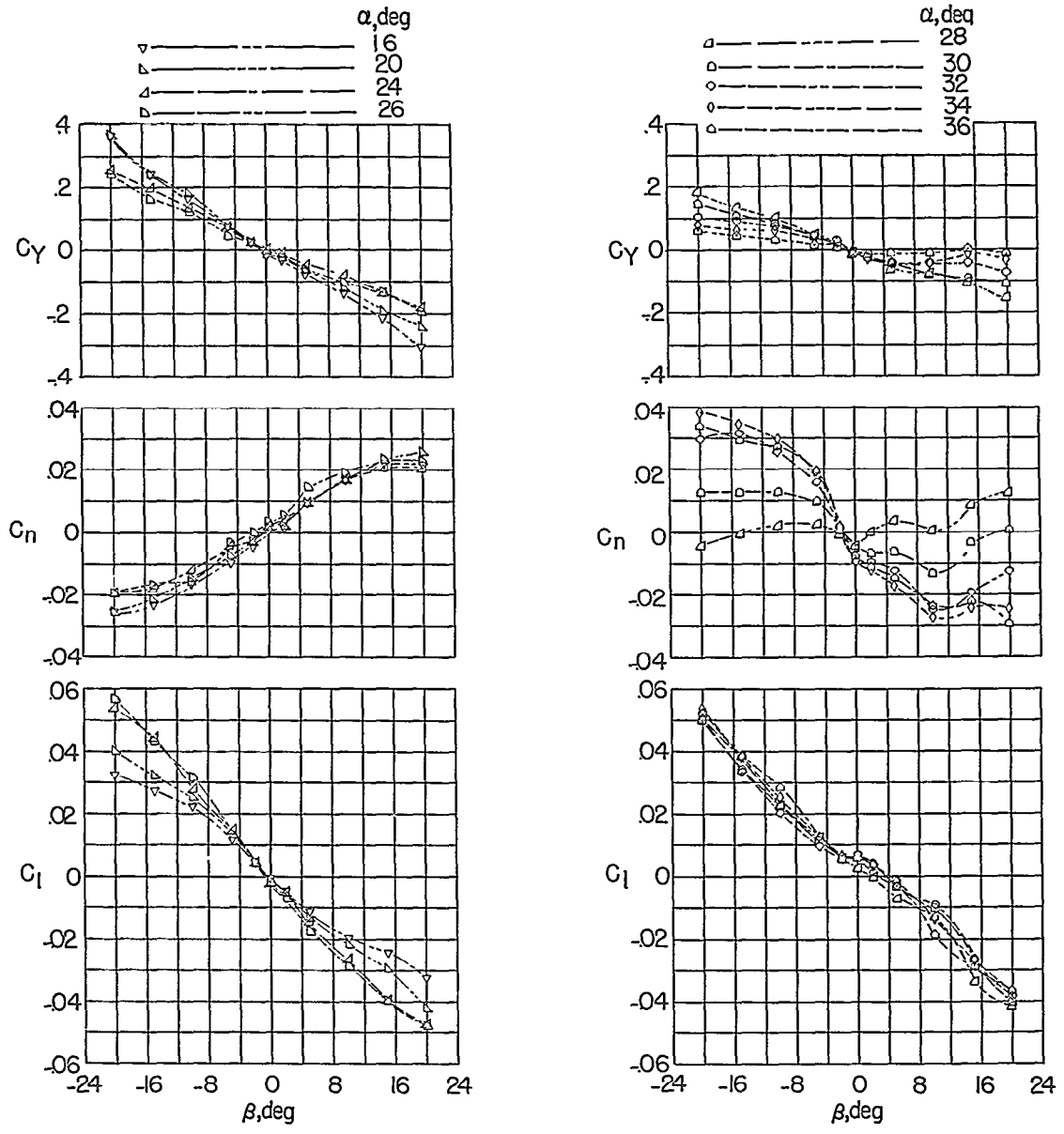

(c) $\frac{S_t}{S} = 0.18$.

Figure 11.- Concluded.

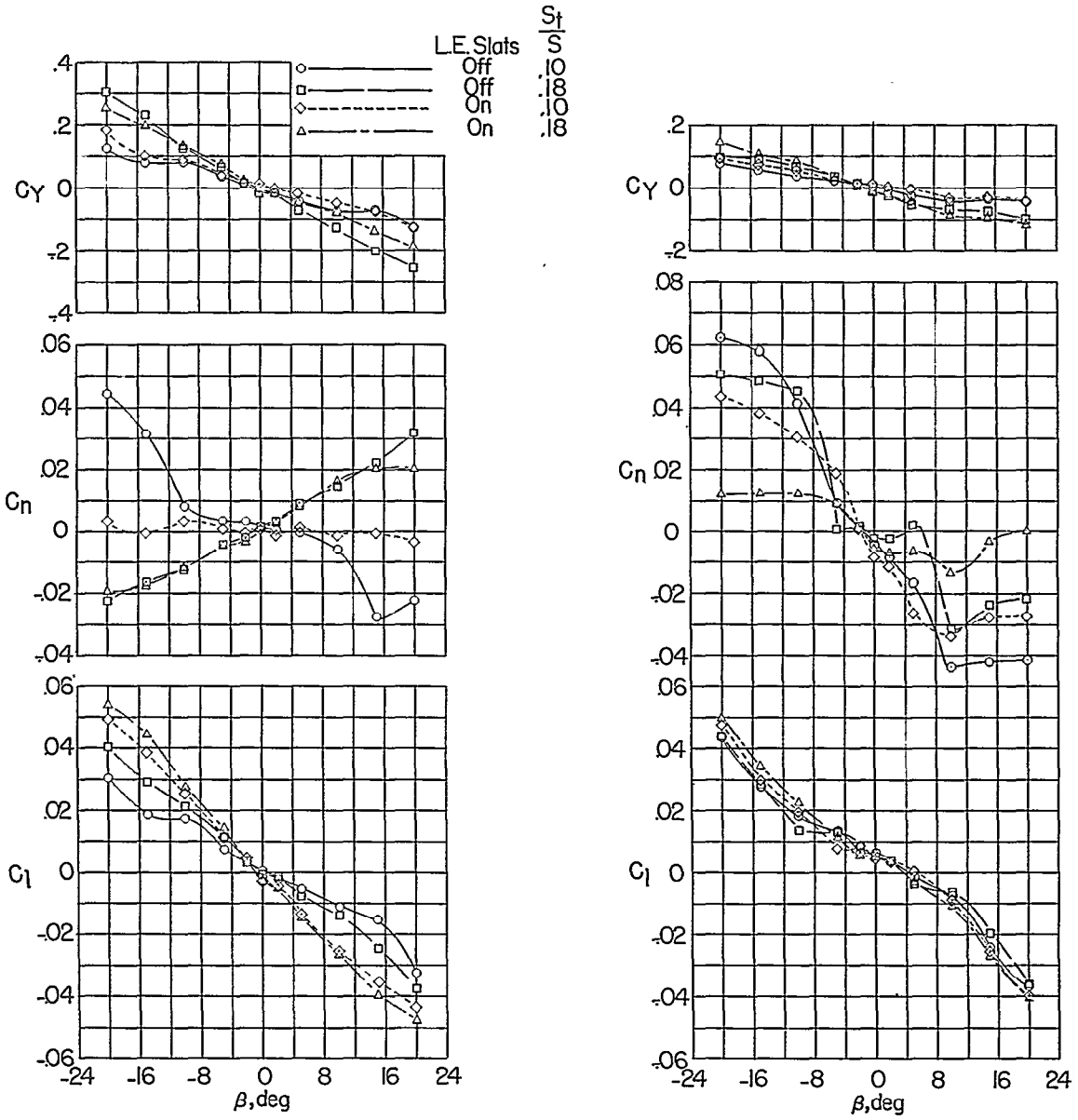

(a) $\alpha = 24^{\circ}$.

(b) $\alpha = 30^{\circ}$.

Figure 12.- Comparison of effects of modifications on the lateral characteristics of the model tested in the Langley free-flight tunnel. $\delta_e = -15^{\circ}$.

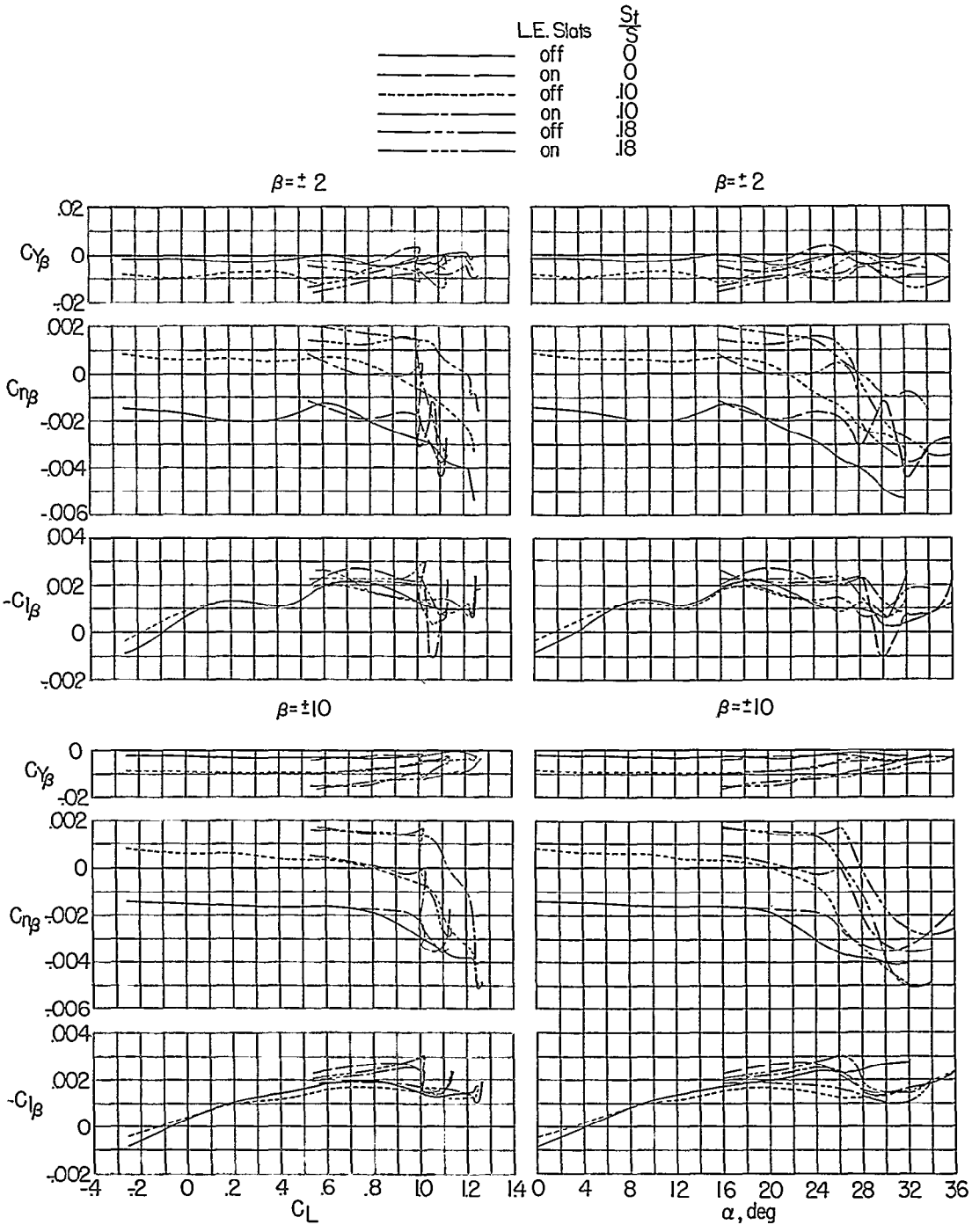

Figure 13.- Lateral-stability parameters of the model tested in the Langley free-flight tunnel. $\delta_e = -15^\circ$.

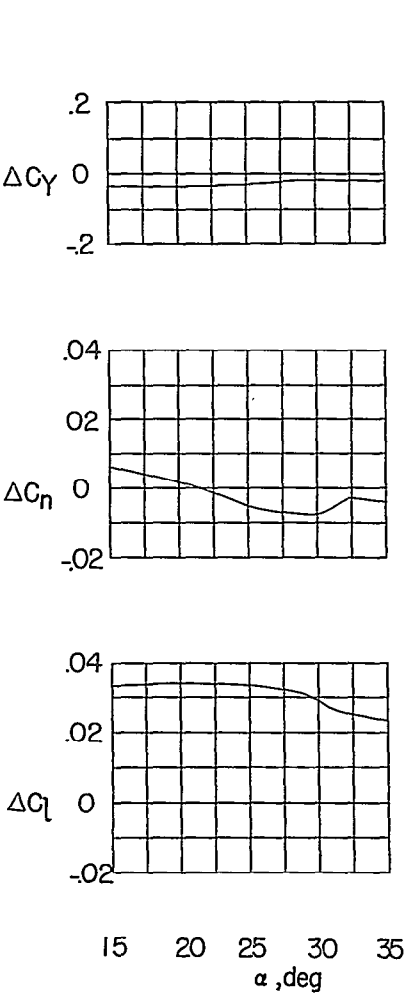

(a) Incremental force and moment coefficients due to aileron deflection. $\delta_a = \pm 15^\circ$.

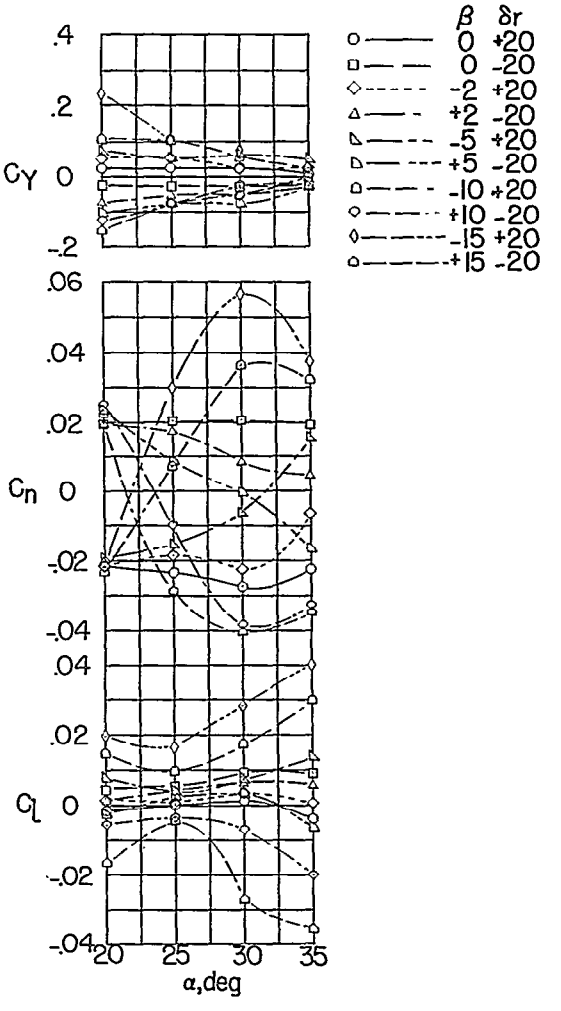

(b) Force and moment coefficients due to rudder deflection.

Figure 14.- Control effectiveness of the model tested in the Langley free-flight tunnel. $\delta_e = -15^\circ$; $\frac{S_t}{S} = 0.10$.

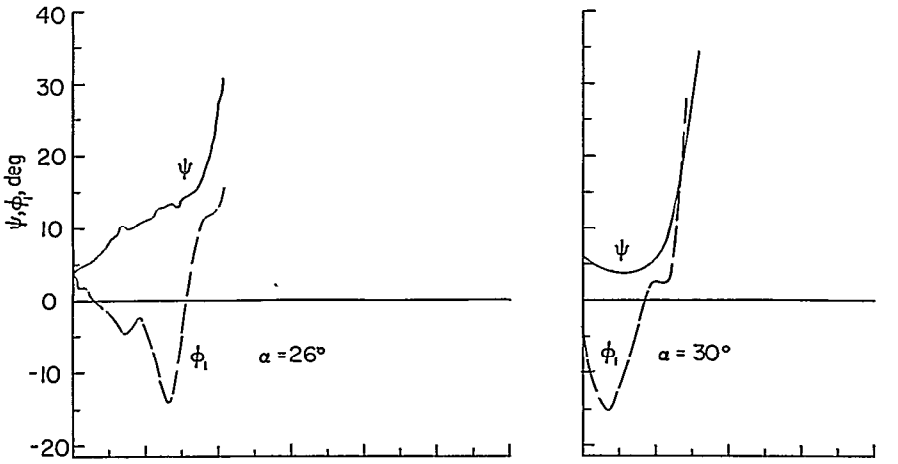

(a) $\frac{S_t}{S} = 0.10$.

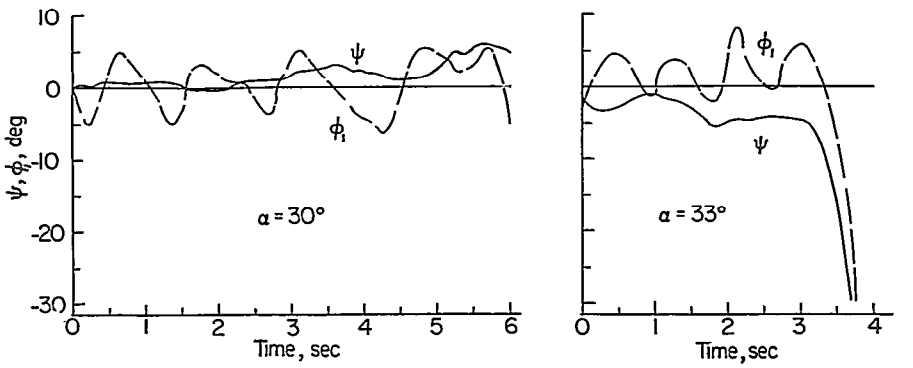

(b) $\frac{S_t}{S} = 0.18$.

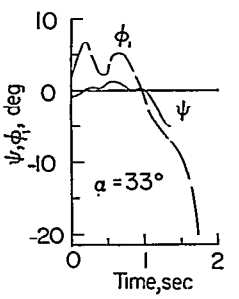

(c) $\frac{S_t}{S} = 0.18$. L.E. slats on.

Figure 15.- Flight records of the model tested in the Langley free-flight tunnel.